Grid Secondary Frequency Control by Fuzzy PI–PD Controller

Ganesh Rapolu[1] and *Padhan* Dola Gobinda[1*], *D*. Chandra Prakash[2], *Muhamed* Hussain[3]

[1]Department of Electrical and Electronics Engineering, Gokaraju Rangaraju Institute of Engineering and Technology, Hyderabad, Telangana, India
[2]KG Reddy College of Engineering & Technology, Hyderabad, Telangana, India.
[3]Department of Refrigeration and air Conditioning Techniques engineering, College of technical engineering, The Islamic University, Najaf, Iraq.

Abstract. This paper develops a new approach for controlling the frequency in a two-area power system using a fuzzy PI PD controller. Frequency stabilization is one of the important factors for any power system to operate efficiently and reliably. The fluctuating characteristics of RES, like solar PV and wind energy, due to changing atmospheric conditions, require additional reserves to compensate for fluctuations in generated power. With growing application of EVs and their charging requirement, charting huge loads may add to the power grid and lead to stability problems if not properly regulated. This paper coordinates EV charging into the secondary frequency regulation, aided by an enhanced fuzzy controller designed for dealing with fluctuating imbalances between electricity demand and generation. In this context, a control technique is suggested that incorporates the flexibility of fuzzy logic with the accurate PI and PD methods for control. The controller continuously monitors changes in frequency at each node in the power system network. The fuzzy logic works on uncertain input data in terms of prescribed linguistic variables and rules that allow it to achieve a reasoned output. The difference between the desired and actual frequencies alters the control variable through the PI component of the controller, while the PD component considers the rate of change of this error to make the system's response time better. The effectiveness of the fuzzy PI PD controller is proven through detailed simulation experiments under different operational conditions and disturbances. It can be rundown that the controller efficiently reduces these frequency deviations, which guarantees smooth and reliable operation of the two-area power system network. In addition, it can be seen that the controller has robust performance but is rather reactive to dynamical changes in system parameters. Case studies are included in the research to test the performance of the proposed control approach in reducing frequency deviations; simulation findings always prove its efficacy. This paper therefore presents a complex method of frequency regulation in power systems using fuzzy logic and combined PI PD control to deal with problems caused by RES integration and EV charging. The proposed technique enhances the frequency stability in order to enhance both the reliability and efficiency of

* Corresponding Author: dgobinda@gmail.com

power grid operations due to the ever-changing energy demands and conditions.

1 Introduction

Frequency control is thus of prime importance for the stable and efficient electricity supply in interconnected multi-area power networks. Further, these deviations in frequency due to generation–load imbalance may result in severe power supply problems and even system-wide blackouts if not timely corrected. Traditional methods, such as Proportional Integral Derivative Control, have been vastly applied in the control of the frequency of power devices. However, this grid has become modern, grown, and nonlinear, hence requiring advanced control systems. Another approach of interest during the past few years has been electric vehicles for frequency control using vehicle-to-grid techniques. Vehicle-to-grid is based on bidirectional converters that connect the batteries within EVs to the grid, allowing them to be charged and quickly discharged in order to modulate grid load and frequency. It assumes that EV batteries can still be useful for providing frequency-related ancillary services since they are always partially charged with respect to typical usage patterns.

Fuzzy logic control has been quite optimistic in practice within power system control, as it makes provisions for handling imprecise and unpredictable data. Making intelligent decisions from qualitative information is possible through fuzzy rules and linguistic variables used by the fuzzy logic controller. This makes it suitable for use in dynamic and complex environments like the power system. This work proposes a new method: a fuzzy proportional integral derivative controller enhanced with PD action for frequency control in two-interconnected power systems. The proposed controller tries to improve the performance in frequency regulation while being resilient and adaptive to changing operating conditions and disturbances. Compared with traditional PID controllers, the fuzzy PI PD controller marries fuzzy logic decision making to the strength and robustness of PI control with the responsiveness of PD action to nonlinear and time-varying dynamics often encountered in modern power systems.

Different research efforts have targeted investigating various control algorithms in controlling the frequency, from simple control using PID to more sophisticated ones, which have utilized artificial intelligence and machine learning. In terms of primary frequency regulation, research powered by electric vehicles demonstrates very promising results with respect to the possibility and manifold advantages of including EVs within grid operations that would stabilize the frequency. While PID controllers have long been applied due to their simplicity and efficiency, fuzzy PI PD controllers have been showing some prospective advantages concerning robustness against parameter variations, speed of response, and disturbance rejection. Further investigation is required to evaluate the applicability in large-scale power networks and the effectiveness of fuzzy PI PD controllers in practice. The advances in AI and control theory further open new research opportunities for the advancement of more sophisticated adaptive control schemes for the improvement in power system frequency regulation. In conclusion, it can be said that the scheme that embodies the benefits of fuzzy logic with PI and PD control actions shows much promise for improving the overall system stability and dynamic response under modern power grid complexities and variability of renewable energy sources and EV integration.

In this paper in the section II System model and the transfer function model diagram with the different energy sources link wind, EV model and SOC estimations are described, in the

Section III the controllers such like fuzzy and Fuzzy PI PD are explained along with their member ship functions and the Rules of the Fuzzy conditions. In the Section IV results and analysis of the proposed system in the different cases with the proposed controllers like fuzzy and fuzzy PI PD.

2 System Modeling

2.1 Studied System

This research assesses the performance of the suggested strategy using the two-area system utilized in [12]. You may get more details about this system's parameters in [7]. Fig. 1 depicts the system in use. The control action signals for primary and secondary control are shown in this figure as ΔPs and ΔPP, respectively. The power changes of the governor, turbine, EVs, and wind power system are shown by Pg, Pm, PEVs, and PW, respectively. In addition, FP is a constant and Tg, Tr, and Tc are generator-turbine time constants. Moreover, the bias factor and speed droop characteristic are represented by R, β, D, and M.

In Fig. 1, ACE_i is the area control error of area I, calculated as follows:

$$ACE_i = B_i \Delta f_i + \Delta P_{Tie,i} \quad (1)$$

where B_i is frequency bias of area I and Δf_i is frequency deviation of area i. $\Delta P_{Tie,i}$ represents the tie line power deviation of area I and is calculated as follows:

$$\Delta P_{Tie,i} = \sum_{\substack{j=1 \\ j\neq 1}}^{N} \Delta P_{tie,ij} = \frac{2\pi}{S}\left[\sum_{\substack{j=1 \\ j\neq 1}}^{N} T_{ij}\Delta f_i - \sum_{\substack{j=1 \\ j\neq 1}}^{N} T_{ij}\Delta f_j\right] \quad (2)$$

where N is the number of areas and T_{ij} denotes the synchronous torque factor be tween regions i and j, which is calculated as:

$$T_{ij} = \frac{|V_i||V_j|}{X_{ij}}\cos\left(\delta_i^0 - \delta_j^0\right) \quad (3)$$

In Eq.3, V_i, δ_i^0, and X_{ij} show area I's terminal voltage, phase, and reactance between area I and j, in that order. The system's basic power has been determined to be 10 MW.

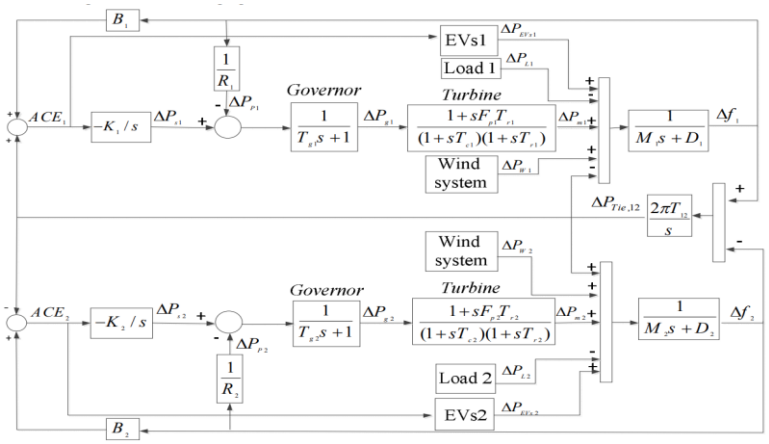

Fig. 1. The studied system.

2.2 Wind Power System

In this work, a random process is used to model wind speed. The wind speed at any given moment $V_\omega(t)$, is wind speed average plus wind speed variations stated as follows [13]:

$$V_\omega(t) = V_{WM} + \sum_{i=1}^{0} A_i \cos(\omega_i t + \Psi_i) \quad (4)$$

where Ai is the amplitude of the variations in wind speed at discrete frequency of and $V_{WM}$is mean wind speed, which is usually calculated as a 10-minute average value of ω_i(i = [1 , 0]), 0 is number of samples and Ψ_i is the random phase angle with the uniform distribution in interval [−π , π]. The spectral density function $S_{(\omega)}$ that is empirically suited to wind turbulence serves as the foundation for the amplitude A_i. This study uses the V_{on}-Karman distribution, which is presented as follows, given by Eq. (5):

$$S_{(\omega)} = \frac{0.475\sigma^2 \frac{L}{V_{WM}}}{\left[1+\left(\frac{\omega L}{V_{WM}}\right)^2\right]^{5/6}} \quad (5)$$

In Equation (5), L represents the turbulence length scale in meters, and σ is wind speed standard deviation. Therefore, using spectral density function of Eq. (5), amplitude of i^{th} harmonic, A_i, is defined as follows:

$$A_i(\omega_i) = \frac{2}{\pi}\sqrt{\frac{1}{2}[S(\omega_i) + S(\omega_{i+1})](\omega_{i+1} - \omega_i)} \quad (6)$$

The wind turbine's power output is as follows: [15]:

$$P_{\omega}(t) = \begin{cases} 0 & V_{\omega}(t) \le V_{Cut-in} \text{ or } V_{\omega}(t) \ge V \\ 0.5\rho\pi R_{wt}^2 C_p(\beta,\lambda) V_{\omega}(t)^3 & V_{Cut-in} < V_{\omega}(t) \le V_{rated} \\ P_{rated} & V_{rated} < V_{\omega}(t) < V_{Cut-off} \end{cases} \quad (7)$$

The wind turbine's output power, denoted as $P_{\omega}(t)$ in Eq. (7), is related to several factors, including air density (ρ), rotor radius R_{wt}^2 performance coefficient C_p, blade pitch angle (β), tip speed ratio (λ), cut-in and cut-off wind speeds V_{Cut-in} and $V_{Cut-off}$, and wind speed at which wind turbine produces its rated power V_{rated}. A pitch angle control system can maintain wind turbine's power output at the rated power when $V_{\omega}(t)$ is between V_{rated} and $V_{Cut-off}$.

2.3 EV Battery Model

In studies on frequency regulation and power system stability, battery storage is represented by transfer function blocks [4]. The voltage source (V_{OC}) in series with the inner resistance R_{series} and the parallel RC network make up, Thevenin-based PHEV battery type [14]. Fig. 2 models the transient overvoltage impact using an RC network. The open circuit voltage, equivalent voltage transient response, and series resistance voltage drop are added to determine the battery terminal voltage ($V_{Battery}$) which is shown in Eq. (8).

$$V_{Battery} = V_{OC} + V_{series} + V_{transient} \quad (8)$$

In this equation, V_{series} is calculated as:

$$V_{series} = R_{series} I_{battery} \quad (9)$$

And Vtransient is obtained as:

$$V_{transient} = \frac{R_t}{1 + sR_tC_t} I_{battery} \quad (10)$$

The Nernst equation is used to model the nonlinear relationship between V_{OC} and battery SOC.

$$V_{OC} = V_{nom} + s\left(\frac{RT}{F}\right) \ln\left(\frac{SOC}{C_{nom} - SOC}\right) \quad (11)$$

where R is gas constant, F is Faraday constant, T is battery temperature, C_{nom} is nominal battery capacity in Ah,
and V_{nom} is nominal voltage. Additionally, s is a sensitivity parameter of V_{OC} to SOC. It is expected that battery and converter have a combined efficiency of 95%. Depending on its sign, Pb in Fig. 2 denotes the battery's input or output power. Bidirectional converters are covered in further detail in [9].

2.3.1 Cell Soc Estimation

The EKF approach is the main technique for estimating cell SoC, as it was stated in the literature study. However, additional study and comparison will also be conducted using the other methodologies.

2.3.2 Coulomb Counting

The algorithm for calculating SoC using coulomb counting is provided in [24]:

$$SoC = SoC_o - \frac{1}{Q_{rated}\int \eta I dt} \quad (12)$$

Where SoC_o is starting value, η is charge-discharge efficiency, and Q_{rated} is rated capacity at the specified temperature and charge-discharge rate.

The anticipated value of SoC at each time can be derived as long as the initial value, as well as the charge and discharge current at each moment, are known.

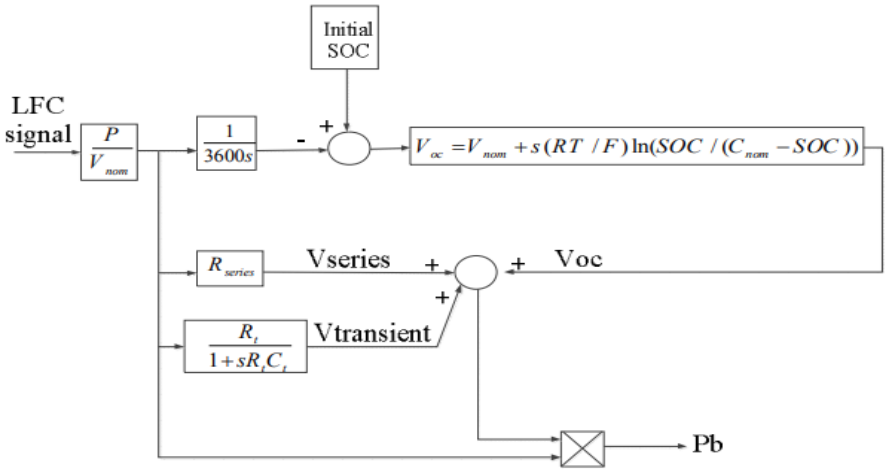

Fig 2. Battery Model.

2.4 LFC Modelling

Determining governor outputs and the controlling their reference operating point are primary objectives of LFC loop. The independent system operator (ISO) states that in order to estimate control area, frequency and total interchange of the power flow are evaluated [12]. The area control error formula is as follows:

$$ACE_i = B_i \Delta f_i + \Delta P_{Tij} \quad (13)$$

For the given two area system, B_1 *and* B_2 the frequency bias coefficients are given by,

$$B_1 = \frac{1}{R_1} + D_1 \quad (14)$$

$$B_2 = \frac{1}{R_2} + D_2 \quad (15)$$

The area control errors ACE_1 and ACE_2 are,

$$ACE_1 = B_1 \Delta f_1 + \Delta P_{tie1} \quad (16)$$

$$ACE_2 = B_2 \Delta f_2 + \Delta P_{tie2} \quad (17)$$

where $\Delta P_{tie1}, \Delta P_{tie2}$ are the tie-line power error transfer for area 1 and area 2.
In general, the equivalent frequency bias factor is expressed as,

$$\beta_{eq} = \sum_{i=}^{n} \frac{1}{R_i} + \sum_{i=1}^{n} D_i \quad (18)$$

Controlling the frequency and tie-line power flow is necessary to keep the power system as secure as possible. Stated differently, the reduction of instabilities resulting from variations in source powers. A PID controller is linked to every generator in order to balance power and keep the system frequency within predetermined ranges.

3 Design of Controller

In order to support secondary frequency management, an improved fuzzy controller is used in this study to regulate the batteries of EVs. Fig. 3 depicts the proposed method's structure. The improved fuzzy controller in this mode receives inputs from the ACE in area I and battery SOC of EV. In this instance, membership functions and fuzzy rules are obtained together with charging and discharging powers. In [8], the fuzzy controller's foundation was explained.

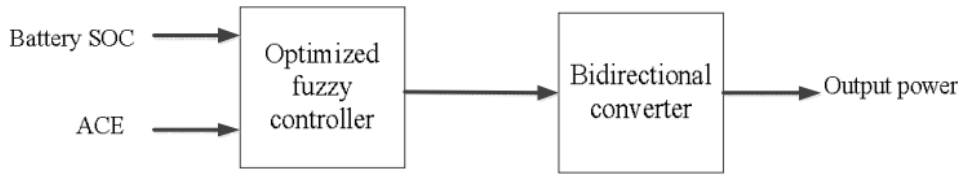

Fig 3. Structure of proposed method.

Fig. 3 shows the proposed method's structure. The variables' membership functions are shown in Fig. 4.
Fig. 4 illustrates the ACE membership function used in this study. The ACE signal is fuzzified into seven linguistic variables: very low (VL), medium low (ML), small low (SL), medium (M), small high (SH), medium high (MH), and very high (VH). These linguistic

variables are defined to appropriately capture the input ACE signal through corresponding fuzzy functions.

Fig. 5 shows the membership functions of the State of Charge (SOC) of the battery, with five linguistic variables: very low, low, medium, high, and very high. These are different fuzzy regions which the SOC input will be divided into to form distinctive qualitative states so that fuzzy logic-based decision-making would be effective. Parameters which aim at optimization are shown through Figs. 4(a) and (b). In the present work, these parameters are tuned for a two-area system by applying step loads to both areas and using the Imperialist Competitive Algorithm. ICA is an efficient and accurate optimization algorithm used in many research papers; its underlying theory is well explained in the literature.
In the process of optimization, constants relating to upper, lower, and middle limits are considered in association with Equation, which acts as the fitness function in this model. The function controls that process of optimization within predefined bounds to ensure that all parameters are suitably tuned for relevant enhancements in the system and increase its stability.

$$F = \int \sum_{i=1}^{E} \left(|\Delta f_i| + \left|\Delta P_{tie,i}\right| \right) tdt \tag{19}$$

Fig. 6: Power membership functions, segmented into nine fuzzy regions linguistically variable: very negative high, negative high, negative medium, negative low, zero, positive low, positive medium, positive high, and very positive high. Linguistic variables are very useful to fuzzify the power input, which varies from fully negative, indicating a fully charged battery, to fully positive high. The membership functions, designed in this work, consider examination and iterative refinement to partition the power variable into quite distinct fuzzy regions. This approach allows the fuzzy logic system to read and respond to changes in the power input over its entire range.

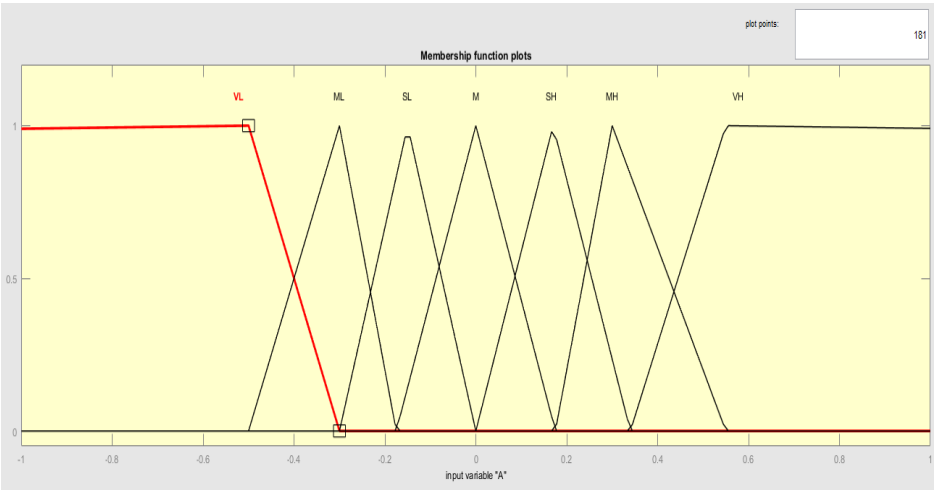

Fig 4. Fuzzy controller membership functions of the Input 1

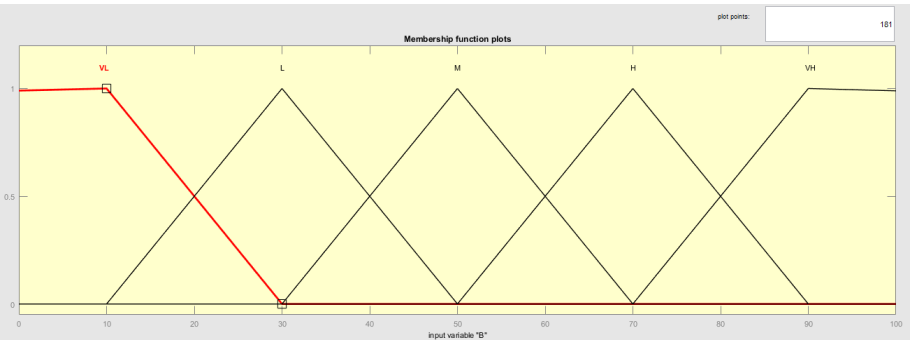

Fig 5. Fuzzy controller membership functions of the Input 2

Table 1 displays the fuzzy controller's fuzzy rules. These guidelines are designed to maintain the battery's SOC at roughly 50%. To keep the battery SOC close to another SOC, these ambiguous regulations can be altered.

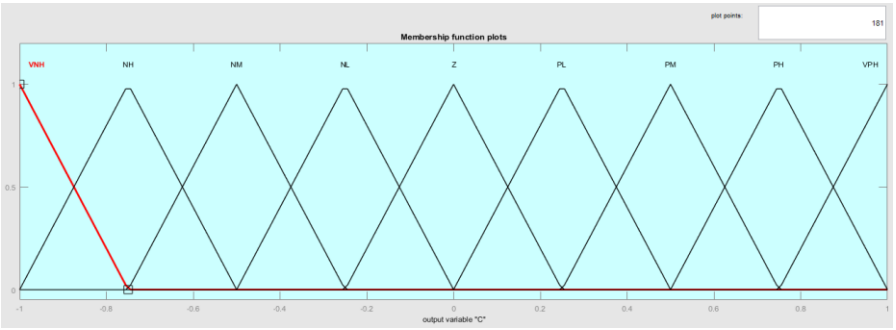

Fig 6. Fuzzy controller membership functions of the output

3.1 Fuzzy Rules and Conditions

TABLE 1. Fuzzy rules and conditions

I/P&O/P MFs	VL	L	M	H	VH
VL	Z	Z	Z	NH	VPH
ML	Z	Z	Z	PH	VPH
SL	Z	Z	Z	PH	PH
M	NL	NL	NL	PH	Z
SH	NM	NM	NM	Z	Z
MH	NH	NH	NH	Z	Z
VH	VNH	Z	PH	NL	Z

4 Results

4.1 Case Study – 1

This study focuses on analyzing a system depicted in Figure 1 to explore the proposed design of a Fuzzy PI-PD controller. Variations in frequency and tie line power are evaluated under

conditions with and without electric vehicles (EVs) engaged in secondary frequency regulation. EVs are assumed to have a power restriction of 3 kW for charging and discharging. The study considers two regions with variable loads. Figures 7(a-b) illustrate frequency deviations in both locations with and without EVs in secondary frequency control. The figures compare frequency irregularities across all areas, showcasing significant reduction when utilizing the suggested Fuzzy and Fuzzy PI-PD controllers.

Figure 8 depicts tie line power deviations. It clearly shows that the proposed controller effectively reduces tie line power deviations. Without EVs, the maximum tie line power deviation in Load Frequency Control (LFC) is 0.03939 pu, whereas with the suggested technique, the maximum deviation is reduced to 0.003911 pu—a 97% improvement. Overall, the results demonstrate that implementing the suggested Fuzzy and Fuzzy PI-PD controllers enhances system performance by mitigating frequency and tie line power deviations effectively.

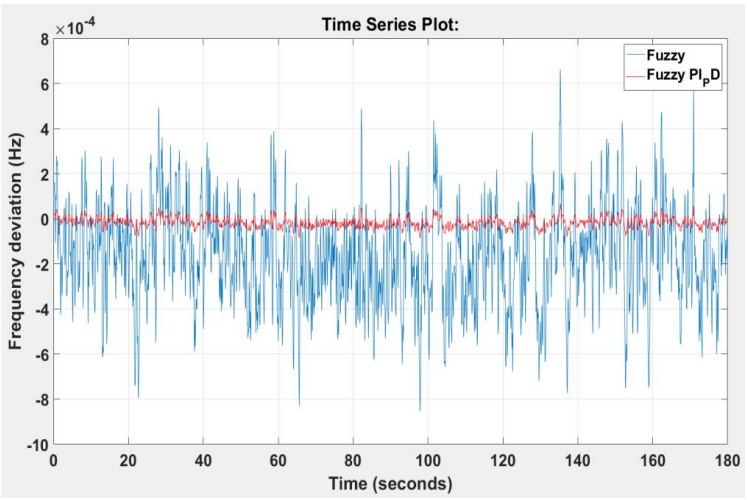

(a)

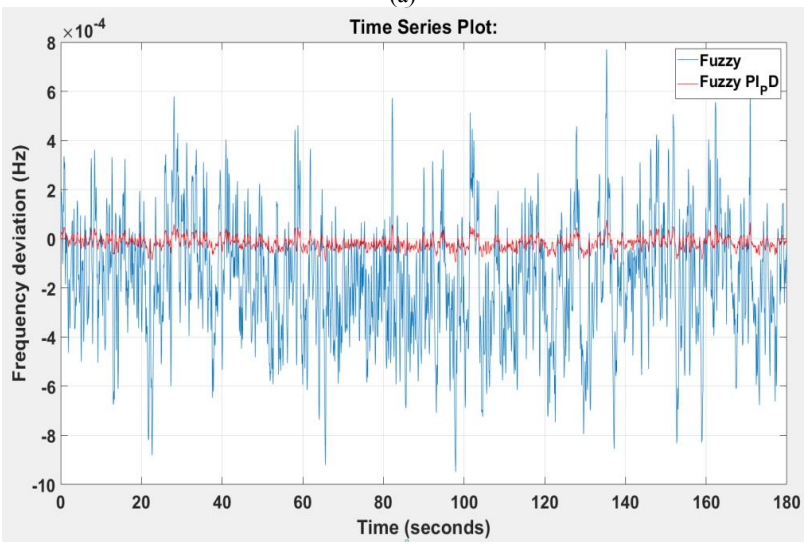

(b)

Fig. 7. Frequency deviation; a) Area 1, b) Area 2.

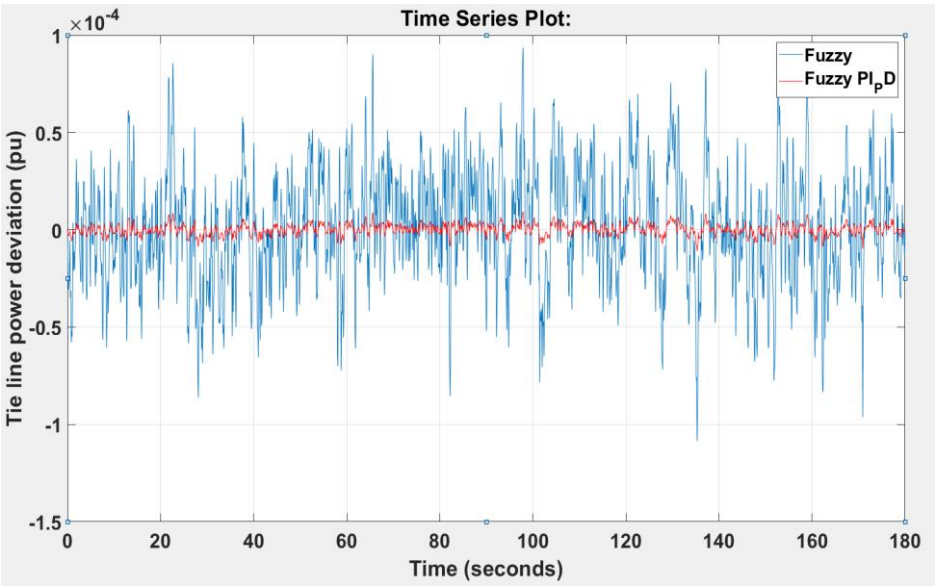

Fig. 8. Tie line power deviation.

4.2 Case Study – 2

Figure 9(a-b) displays the area control error (ACE) for regions 1 and 2, comparing scenarios with and without the proposed strategy. As expected, the application of the proposed strategy leads to a substantial decrease in ACE for both regions.

4.3 Case Study – 3

Fig.10 demonstrates the performance of the suggested Fuzzy PI-PD approach under heavy load conditions. In this case study, region 1 experiences a load disturbance of 0.01 pu at 20 seconds. The figure illustrates that utilizing the suggested method results in a reduced maximum frequency deviation for region 1 compared to when it is not employed.

4.4 Case Study – 4

In this study, the traditional plants' fuzzy controller generates the Load Frequency Control (LFC) signal. Figures 11(a-b) depict frequency variations in Area 1 and Area 2. These figures clearly demonstrate that the proposed method outperforms the fuzzy controller in reducing frequency deviations in both areas.

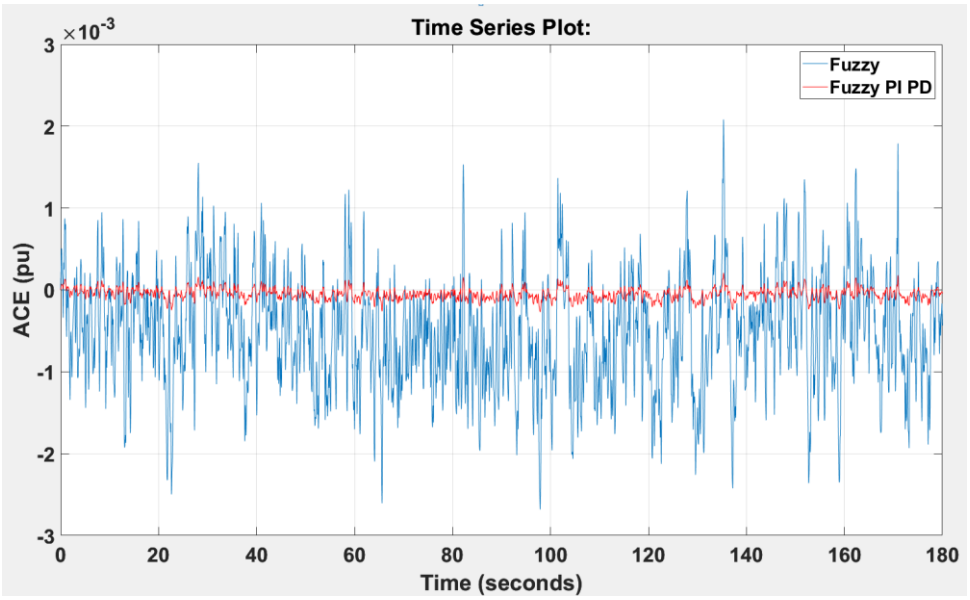

(a)

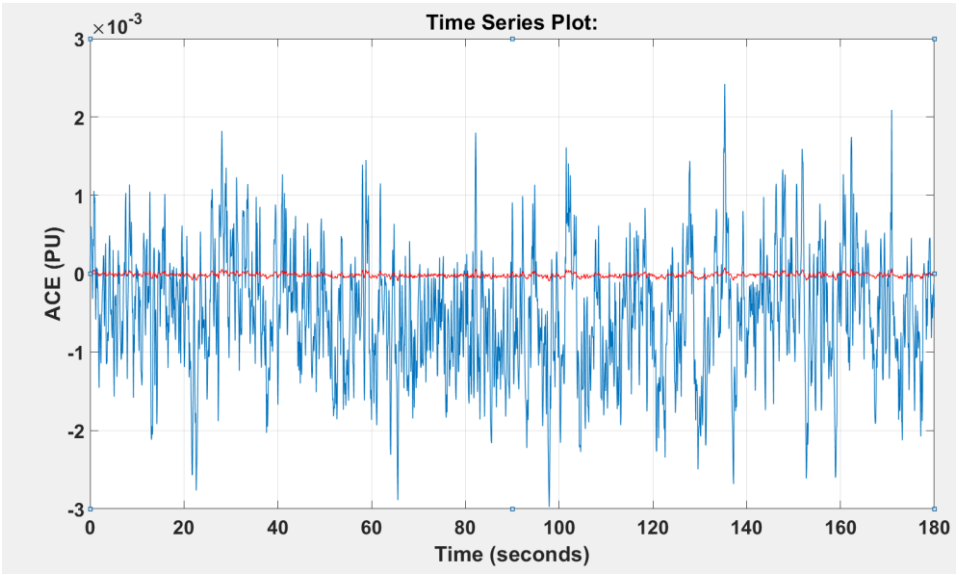

(b)

Fig 9. ACE a) Area 1,b) Area 2

(a)

(b)

Fig. 10. A zoomed view of area 1's frequency deviation after applying a 0.1 pu load a) Area 1, b) Area 2.

For instance, the maximum frequency deviations in Area 1 and Area 2 using the proposed method are 0.0001302 Hz and 0.0001543 Hz, respectively. In contrast, when using the fuzzy PI-PD controller, the maximum frequency deviations are 0.000001289 Hz and 0.000001532 Hz for Area 1 and Area 2, respectively. Furthermore, it is observed that the suggested approach surpasses the PI controller in reducing tie line power deviations.

4.5 Case Study – 5

In this case study, due to the expected total power of electric vehicles (EVs) potentially surpassing the grid capacity, overregulation could occur. To mitigate this issue, the output power of EVs is capped at a specified limit. According to the assumptions, Region 2 has 2,000,000 EVs and Area 1 has 3,000,000 EVs. Figures 12(a-b) illustrate frequency variations. In this scenario, there is an excess of regulation. Therefore, a limiter is introduced with upper and lower bounds set at 10,000 kW each. It is found that when the suggested approach is used alongside the limiter, it performs better compared to when the limiter is not employed.

4.6 Performance Indices

To optimize the PID, the following cost functions or performance indices have been used as minimization criteria to adjust the PID:

$$IAE = \int_0^t (\Delta f_1 + \Delta f_2 + \Delta P_{tie})\, dt \quad (20)$$

$$ISE = \int_0^t \left(\Delta {f_1}^2 + \Delta {f_2}^2 + \Delta {P_{tie}}^2\right) dt \quad (21)$$

$$IATE = \int_0^t (\Delta f_1 + \Delta f_2 + \Delta P_{tie})\,(t)dt \quad (22)$$

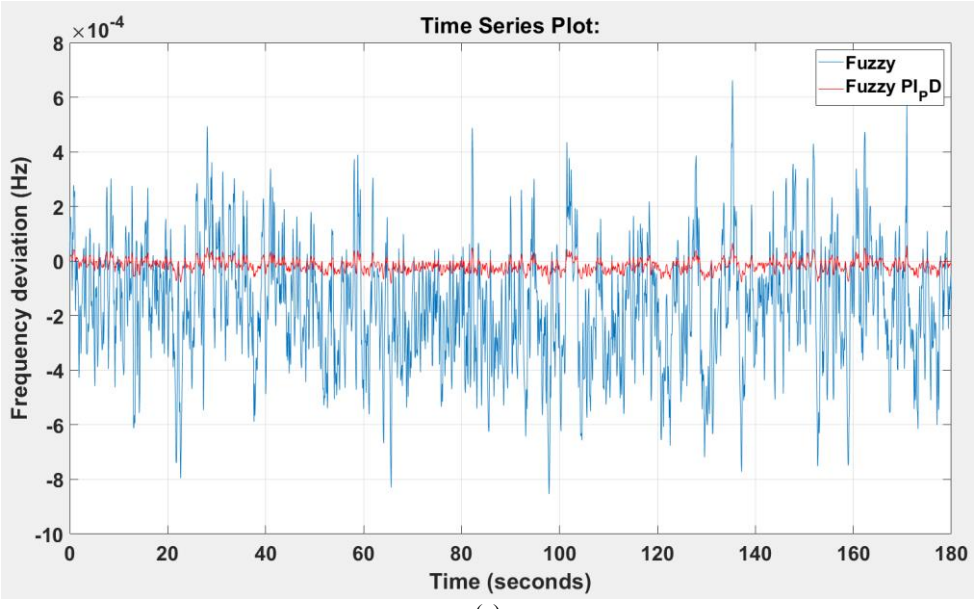

(a)

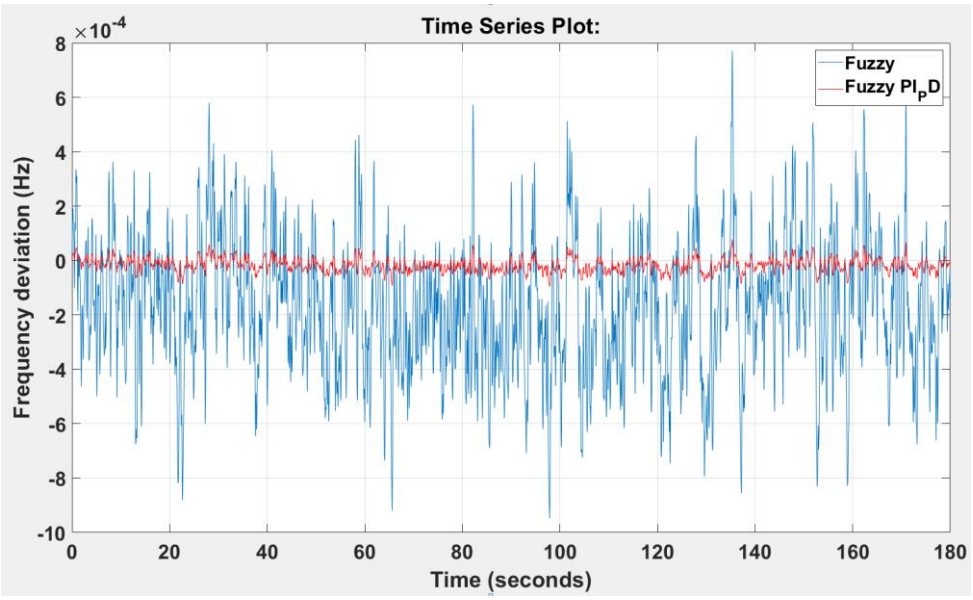

(b)

Fig. 11. Frequency deviation with the proposed approach Fuzzy PI PD and Fuzzy controller; a) Area 1, b) Area 2.

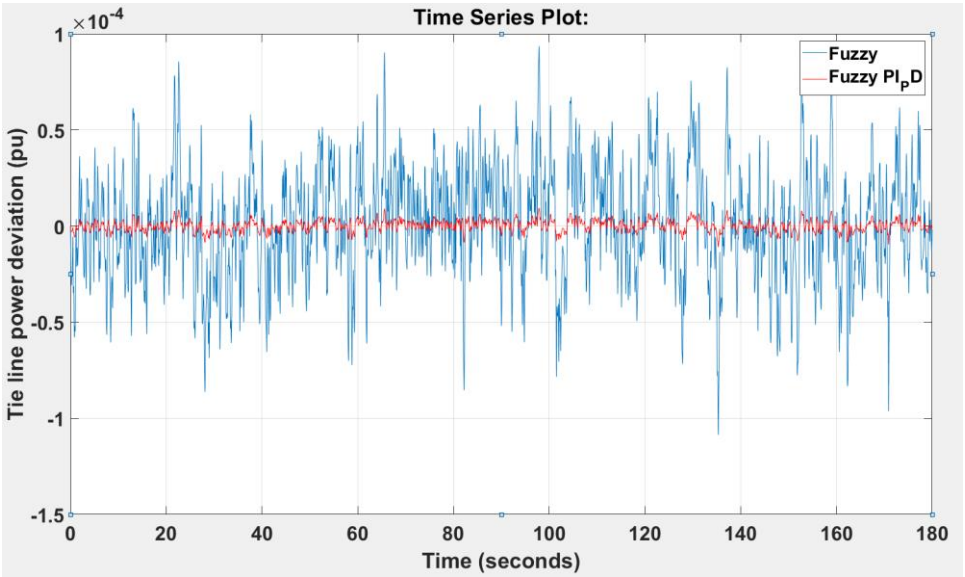

Fig. 12. Tie line power deviation using the proposed approach. Fuzzy PI PD and Fuzzy Controller

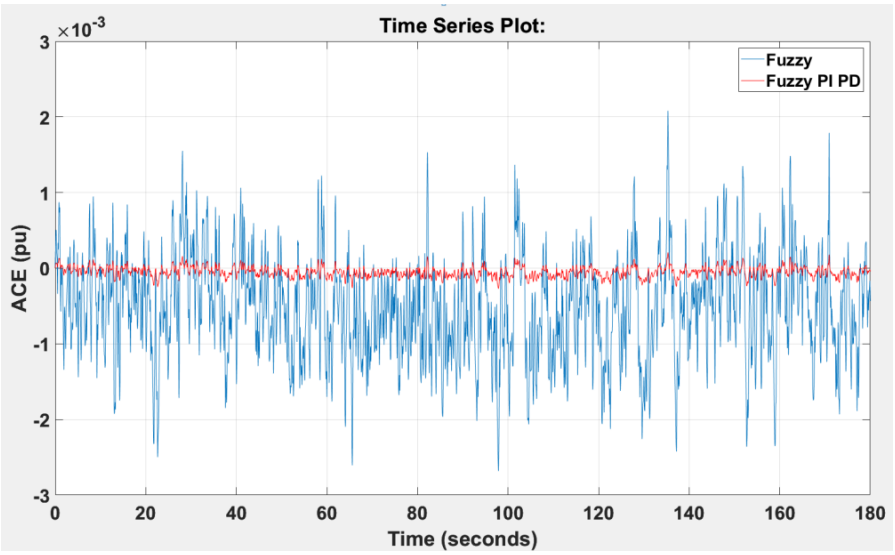

(a)

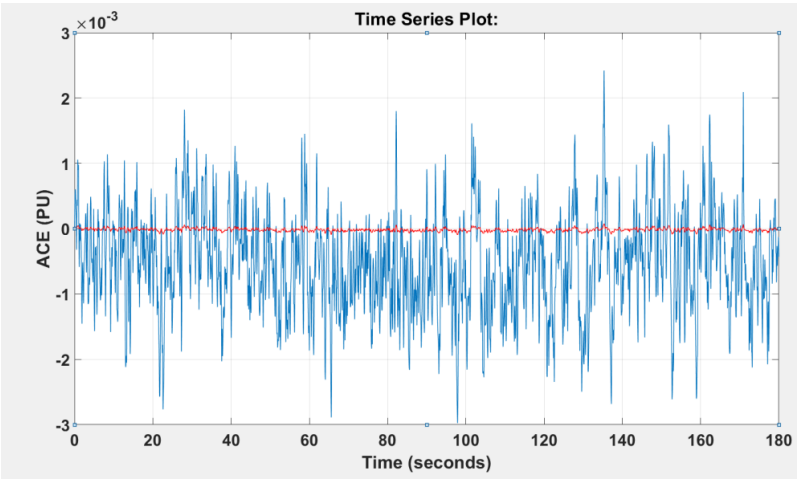

(b)

Fig. 13. ACE with the proposed approach Fuzzy PI PD and Fuzzy controller; a) Area 1, b) Area 2.

Table 2. Area wise IE, IAE, ISE, ITAE and ITSE

	Indices	**PI**	**FUZZY**	**FUZZY PI_PD**
Area 1	IE	0.04217	0	0
	IAE	2.045	0.03939	0.003911
	ISE	0.03704	0.0001302	0.000001289
	ITAE	188.2	3.644	0.3653
	ITSE	5.424	0	0
Area 2	IE	0.07964	0	0
	IAE	2.253	0.04	0.004237
	ISE	0.04489	0.0001543	0.000001532
	ITAE	207.4	3.94	0.3943
	ITSE	11.13	0	0

5 Conclusion

In this paper, a new technique of frequency regulation in two-area systems using a fuzzy PI PD controller has been proposed. Proper frequency control at each operating point is one of the important components of power system performance, and dependable and efficient supply of energy is dependent on it. In this paper, a new approach to EV-based secondary frequency management, based on the V2G idea, was presented. In this approach, it is the optimized fuzzy PI PD controller that had control over the electric vehicles. The proposed controller integrates the different aspects of fuzzy logic with PI and PD control actions to provide an effective solution to the issues related to frequency regulation in the modern grid. The controller is, therefore, suitable for complex and dynamic systems like power systems because it can handle the uncertainties and imprecisions in the input data through fuzzy logic-based decision-making. Simulation experiments can prove that the fuzzy PI PD controller is very competent in controlling the frequency deviations in a two-area power system under various operating conditions and disturbances. The result indicates that the controller exerts better performance than the conventional PID controllers on the three performance indices: robustness, disturbance rejection, and dynamic responsiveness. In case the system is left without a control, the very high percentage overshoot and long settling time will depict poor response. The adoption of the suggested swarm intelligence-based algorithms increases the response of the system to a higher percentage. This formed a strongly converging stable system with improved metrics in the system criteria as rise time, percentage overshoot, settling time, steady state error, and cost functions like IAE, ISE, and ITAE.

References

1. M. D. Galus, S. Koch, G. Andersson, “Provision of load frequency control by PHEVs, controllable loads, and cogeneration unit,” IEEE Trans. Industrial Electronics, vol. 58, no. 10, pp. 4514–4525, October, 2011.R. T. Wang, “Title of Chapter,” in *Classic Physiques*, edited by R. B. Hamil (Publisher Name, Publisher City, 1999), pp. 212–213.
2. A. Dán, C. Farkas, L. Prikler, “V2Geffects on frequency regulation and under-frequency load shedding in a quasiislanded grid”, PowerTech, 2013 IEEE Grenoble, pp. 1 – 6, 2013. B. R. Jackson and T. Pitman, U.S. Patent No. 6,345,224 (8 July 2004)
3. R. Garcia-Valle, J. A. Pecas Lopes, “Electric vehicle integration into modern power networks”,1 st ed., New York: Springer, 2013.
4. J. R. Pillai, “Electric vehicle based battery storages for large scale wind power integration in Denmark,” PhD dissertation, Dept. Energy Technology, Univ. Aalborg, Denmark, December 2010.
5. W. Kempton, S.E. Letendre. “Electric vehicles as anew power source for electric utilities,” Transp. Res. D.,vol. 2, no. 3, pp. 157-175, Sep. 1997.
6. W. Kempton, J. Tomic, “Vehicle-to-grid power fundamentals: calculating capacity and net revenue,” Power Sources, vol. 144, no. 1, pp. 268–279, Jun. 2005.
7. H. Bevrani, “Robust power system frequency control”, 2nd Ed., New York:Springer, 2013.
8. S. Falahati, S. A. Taher, M. Shahidehpour, “A new smart charging method for EVs for frequency control of smart grid”, International Journal of Electrical Power & Energy Systems, vol. 83, pp. 458-469, December 2016.
9. S. Falahati, S. A. Taher, M. Shahidehpour, “Smart deregulated grid frequency control in presence of renewable energy resources by EVs charging control”, IEEE Trans. on Smart Grid, article in press, 2016.

10. T. Masuta, A. Yokoyama, “Supplementary load frequency control by use of a number of both electric vehicles and heat pump water heaters,” IEEE Trans. on Smart Grid, vol. 3, no. 3, pp. 1253 – 1262, September 2012.
11. M. Datta, T. Senjyu, “Fuzzy control of distributed PV inverters/energy storage systems/electric vehicles for frequency regulation in a large power system,” IEEE Trans. Smart Grid, vol. 4, no. 1, pp. 479 – 488, March 2013.
12. J. Zhong, L. He, C. Li, Y. Cao, J. Wang, B. Fang, L. Zeng, G. Xiao, “Coordinated control for large-scale EV charging facilities and energy storage devices participating in frequency regulation,” Applied Energy, Vol. 123, pp. 253–262, 2014.
13. A. F. Zobaa, R. C. Bansal, “Handbook of Renewable Energy Technology”,1 st Ed. World Scientific Publishing, 2011, pp. 45-46.
14. X. Luo, Sh. Xia, K. W. Chan, “A decentralized charging control strategy for plug-in electric vehicles to mitigate wind farm intermittency and enhance frequency regulation”, Journal of Power Sources, Vol. 248,pp. 604-614, 2014.
15. E. Atashpaz-Gargari, C. Lucas, “Imperialist competitive algorithm: An algorithm for optimization inspired by imperialistic competition,” IEEE Congress on Evolutionary Computation 2007, pp. 4661–466, 2007.